Marine Chemistry 196 (2017) 1–12

Contents lists available at ScienceDirect

Marine Chemistry

journal homepage: www.elsevier.com/locate/marchem

Seasonal variations in C:N:Si:Ca:P:Mg:S:K:Fe relationships of seston from Norwegian coastal water: Impact of extreme offshore forcing during winter-spring 2010

Svein Rune Erga[a,*], Stig Bjarte Haugen[a], Gunnar Bratbak[a], Jorun Karin Egge[a], Mikal Heldal[a], Kjell Arne Mork[b], Svein Norland[a]

[a] Department of Biology, University of Bergen, PO Box 7803, N-5020 Bergen, Norway
[b] Institute of Marine Research, PO Box 1870 Nordnes, 5817 Bergen, Norway

ARTICLE INFO

Keywords:
Elemental ratios
Seston
Physical forcing
Norwegian coastal water

ABSTRACT

The aim of this study was to reveal the relative content of C, N, Ca, Si, P, Mg, K, S and Fe in seston particles in Norwegian coastal water (NCW), and how it relates to biological and hydrographic processes during seasonal cycles from October 2009–March 2012. The following over all stoichiometric relationship for the time series was obtained: $C_{66}N_{11}Si_{3.4}Ca_{2.3}P_1Mg_{0.73}S_{0.37}K_{0.35}Fe_{0.30}$, which is novel for marine waters. A record-breaking (187-year record) negative North Atlantic Oscillation (NAO) index caused extreme physical forcing on the Norwegian Coastal Current Water (NCCW) during the winter 2009–2010, and the inflow and upwelling of saline Atlantic water (AW) in the fjord was thus extraordinary during late spring-early summer in 2010. The element concentrations in fjord seston particles responded strongly to this convection, revealed by maximum values of all elements, except Fe, exceeding average values with 10.8 × for Ca, 9.3 for K, 5.3 for S, 5.1 for Mg, 4.6 for Si, 4.0 for P, 3.8 for C, and 3.3 for N and Fe. This indicates that the signature of the Atlantic inflow was roughly two times stronger for Ca and K than for the others, probably connected with peaks in coccolithophorids and diatoms. There is, however, 1.5 × more of Si than Ca contained in the seston, which could be due to a stronger dominance of diatoms than coccolithophorids, confirming their environmental fitness. In total our data do not indicate any severe nutrient limitation with respect to N, P and Fe, but accumulation of iron by Fe-sequestering bacteria might at times reduce the availability of the dissolved Fe-fraction. There is a high correlation between most of the measured elements, except for Ca, which together with Fe only weakly correlated with the other elements. It is to be expected that environmental alterations in NCW related to climate change will influence the seston elemental composition, but the full effect of this will be strongly dependent on the future dominance of the high pressure versus low pressure systems (i.e. NAO index), since they are key regulators for the direction of wind driven vertical convection (i.e. upwelling or downwelling). Changes in stratification, temperature, light, pH (ocean acidification), $CaCO_3$ concentrations (carbon pump) and availability of nutrients in the euphotic zone (biogeochemical cycling) are essential for the future dominance of coccolithophorids versus diatoms.

1. Introduction

Seston comprises living plankton, organic detritus and inorganic particles, and its elemental and biochemical composition is important not only for the food requirements of grazers and suspension feeders, but also for the energy transfer in the food chain and for the understanding of the nutrient dynamics and primary production of aquatic ecosystems, including growth control (Sterner and Hessen, 1994; Navaro and Thompson, 1995; Ho et al., 2003; Price, 2005). The composition is highly variable, both qualitatively and quantitatively. While phytoplankton is the main contributor during blooms, bacteria and grazers, including heterotrophic flagellates, protozoa and micro-zooplankton, dominate towards the end of the blooms and inorganic particles after the bloom (Cranford and Hargrave, 1994; Navaro and Thompson, 1995; Larsen et al., 2004; Erga et al., 2005). In connection with heavy rainfall and snow melt, large quantities of detritus and dissolved organic matter of terrestrial origin are entering fjord and coastal waters (Erga et al., 2005; Erga et al., 2012). Besides this, crustal enrichment (e.g. sediment resuspension) could be a source for particulate matter in the water masses during periods of convection

* Corresponding author.
E-mail address: svein.erga@uib.no (S.R. Erga).

http://dx.doi.org/10.1016/j.marchem.2017.07.001
Received 9 September 2016; Received in revised form 12 June 2017; Accepted 7 July 2017
Available online 12 July 2017

(upwelling) (Stabholz et al., 2013), but the effect of this on the upper part of the water column is strongly dependent on water depth.

Phytoplankton play a key role in the carbon-C cycle of the oceans, contributing with 50% of the global biological uptake of carbon dioxide through primary production, by which particulate organic carbon (POC) and/or inorganic carbon as calcium carbonate are formed. Among the phytoplanktoners, diatoms, having silicate-Si as the major structural component of the outer cell wall (frustule), constitute > 40% (i.e. 20% of the global primary production) (Buchan et al., 2014). This makes them the most important plant group on earth, and Si as a key regulating factor for the function of marine aquatic ecosystems. In addition, other planktoners like radiolarians and silicoflagellates, both containing a silicate skeleton, could make their contribution to the particulate Si-fraction of marine waters (Lange et al., 1997).

The seston as a whole is fundamental for the biogeochemical cycling and bioavailability of macro and micro elements (Bratbak et al., 1992; Zwolsman and van Eck, 1999; Arrigo, 2005). Among these, nitrogen (N) and phosphorous (P) are essential macronutrients for growth of bacteria and phytoplankton in general (Arrigo, 2005). Sulfur is known as a major constituent of amino acids, proteins, enzymes, sulfolipids, and a number of other biochemical compounds (Haines, 1973; Taiz and Zeiger, 2006), but very little is known about S-acquisition in marine phytoplankton (Giordano et al., 2005).

The major cations K, Mg and Ca are important as cofactors for many plant enzymes, and in addition Mg takes part in phosphate transfer, and is also an important constituent of the chlorophyll molecule (Taiz and Zeiger, 2006). In both plant cells and marine archaea, high internal concentration of K^+ seems to be closely connected to osmoregulation (Martin et al., 1999; Taiz and Zeiger, 2006), and in marine bacteria Mg^{2+} has been ascribed a similar role (Heldal et al., 2012a). In plant cells the vacuole with its content of cations, among which K, Mg and Ca are essential, and anions, play a key role in osmoregulation. Even if potassium is not incorporated into organic matter in plants, its concentration is relatively high due to its important role in many physiological processes (Tůma et al., 2004). In diatoms the vacuole/s constitutes a much larger part of the total cell volume than for other phytoplankton types, in some cases it amounts to 60% (Sicko-Goad et al., 1977). In calcifying plankton organisms, like coccolithophores and foraminifera, the concentration of Ca is very high in their cell wall structures (as calcium carbonate) (von Bodungen et al., 1995). The coccolithophore *Emiliania huxleyi*, which make dense blooms, is known as being one of the most important calcium carbonate producers on earth (Westbroek et al., 1993). Particulate Ca, K and Mg can also be transported in the form of aerosols into some marine areas (Fomba et al., 2014).

Within the group of essential trace elements, Fe is a major component of cytochromes and an important cofactor of enzymes in many metabolic pathways of protists and bacteria, and has been reported to be limiting primary production in many oceanic environments (Kolber et al., 1994; Wells et al., 1995; Seeber, 2002). Fe and Mn sequestering bacteria have in addition been suggested to be of quantitative importance for the cycling of these elements in some coastal ecosystems (Heldal et al., 1996b).

The pioneer work of Price and Skei (1975), provided new knowledge on the chemistry of suspended particulate matter, including their content of Si, Al, Ti, Ca, Mg, Fe, Mn, K, P, and S, along a fjord gradient (i.e. from head to mouth) in the Hardangerfjord, western Norway. In another comprehensive study focusing on trace element composition of suspended particulate matter of the eastern North Atlantic, Barrett et al. (2012) obtained valuable information on their spatial distribution. The role of anthropogenic and natural origin of particulate trace elements in high latitude coastal waters was investigated by Bazzano et al. (2014) in the Kongsfjord, Svalbard.

Even if N and P are considered to be among the most essential elements for primary production in the oceans, more information about the role of other elements are needed to improve our understanding of nutrient transfer and biogeochemical cycling at the lower trophic levels of the food chain. Our expanded list of elements comprises C, N, Ca, Si, P, Mg, K, S and Fe, which have been studied frequently during the period October 2009–March 2012 in the Raunefjord, an open coastal fjord in western Norway, adjacent to the North Sea. The location of the study site is strategic with respect to linking inshore-offshore waters. Due to the importance of wind driven water exchanges for seston composition and biomass, and for the question of its autochthonous and/or allochthonous origin, these aspects have been especially addressed together with the effect of a record-breaking (187-year record) negative NAO index during the winter 2009–2010. As far as we are aware such extended time-series are novel for marine waters. They are important not only for establishing seasonal ranges of elemental composition of particulate matter, but also for determining what element is potentially limiting primary growth.

2. Material and methods

2.1. Study sites

The present investigation took place in the Raunefjord, which is situated on the west coast of Norway, south of the city of Bergen (Fig. 1). It is 15 km long north-south oriented fjord, connecting with the open coastline, to the south via the deep Korsfjord (east-west oriented), and to the north via the Hjeltefjord. The Raunefjord is also connected with fjord systems penetrating further inshore at both the north and south ends. The sill depths are 114 m in the south and 90 m in the north. A maximum depth of 240 m is found on the western side. The sampling station, 60°16.19′N, 05°11.41′E, was situated in the eastern part (depth < 130 m) (Fig. 1). In addition, offshore hydrographical data were collected on east-west going cruises along the Fedje-Shetland transect. The stations are typically covering the NCCW from the coastal island Fedje (positioned just north of the Raunefjord) and westwards across the Norwegian trench (300–350 m), and further into the more shallow (100 m) North Sea/Atlantic water (Fig. 1).

2.2. Sampling and analysis

The seston sampling program in the Raunefjord was carried out with R/V “Aurelia” from 13 October 2009 to 19 March 2012. Water for elemental compositing of seston was collected at weekly to bi-weekly intervals from 5 m depth using 2.5 L Niskin water bottles. Samples for dissolved inorganic nutrients and chl *a* were collected in addition during spring and early summer in 2010. The adjacent offshore waters were sampled on two Fedje-Shetland cruises with R/V “Håkon Mosby” on 25–27 February and 4–5 May 2010. On these cruises water samples for chl *a* and nutrients were collected at discrete depths using 5 L Niskin bottles mounted on a rosette sampler.

The hydrographical parameters and in situ fluorescence and turbidity were obtained by calibrated CTDs (Conductivity-Temperature-Depth), a SAIV-SD 204 in the Raunefjord, and a Seabird SBE 911 probe mounted on a General Oceanic Rosette in the North Sea. The CTD temperature sensor was calibrated before the cruises, and the salinity was calibrated by analysing the samples collected routinely from the water bottles at the deepest sampling level on each cast. These analyses were conducted using a Guildline 8400 AutoSal with IAPSO Standard Sea Water as a reference. The turbidity was measured as backscattering at 880 nm. Wind data from Slåtterøy lighthouse, situated to the southwest and adjacent to the North Sea (Fig. 1), were obtained from the Norwegian Meteorological Institute's climate data base “eKlima” (http://eklima.met.no).

Samples for chl *a* determination were filtered onto 25 mm GF/F filters and stored at − 20 °C before analysis within 2 weeks. After thawing the filters, chl *a* was extracted by using 90% acetone as solvent. Concentrations were measured fluorometrically (Turner Designs-10) with acid corrections for phaeopigments according to Parsons et al.

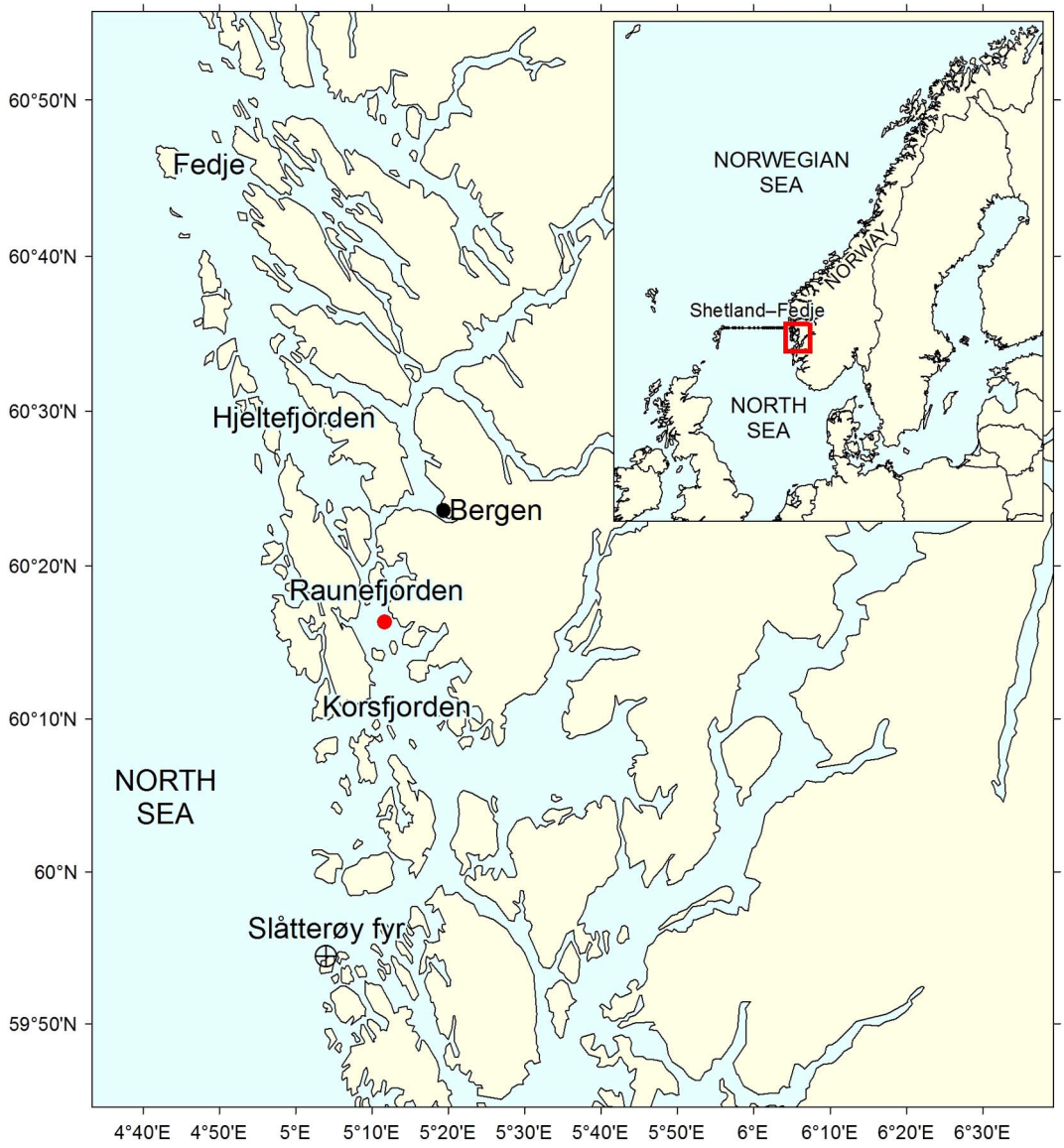

Fig. 1. Map of the investigation area. The location of the study site in the Raunefjord is shown by the red dot, the Fedje-Shetland transect by the black dotted line (coarse scale insert) and the Slåtterøy lighthouse by the encircled cross. (For interpretation of the references to color in this figure legend, the reader is referred to the web version of this article.)

(1992). Nutrient samples (nitrate, nitrite, orthophosphate, silicate) were preserved with chloroform, kept refrigerated and analysed according to standard methods (Parsons et al., 1992) adapted to an autoanalyser from Chemlab Instruments (Rey et al., 2000).

Water samples (250–1500 mL) for qualitative and quantitative analysis of the elemental composition of seston were filtered in triplicate onto 0.6 μm pore size Poretics polycarbonate (PC) filters (47 mm), and 0.6–0.8 μm nominal pore size Whatman GF/F glass fiber filters (47 mm). Even if PC pore size of 0.4 μm is often used to collect suspended particulate matter (SPM) in other studies (Barrett et al., 2012; Bazzano et al., 2014), we selected 0.6 μm pore size to be able to compare it with the elements harvested on GF/F filters. The filters were rinsed with 5 mL of reverse osmosis water to avoid salt precipitations; air dried and stored in Millipore petri slides until analysis. The waters samples were thoroughly mixed before subsampling and filtration, and care was taken to avoid particulate contamination by rinsing sample containers, measuring cylinders, filter holders etc. with sample water before use. It should be noted that the risk of significant contamination of particulate material is considered to be much less than when working with dissolved compounds.

The filters were analysed using a wavelength dispersive X-ray fluorescence (WDXRF) spectroscopy technique adapted for marine samples in a Bruker AXE S4 Pioneer WDXRF instrument (Paulino et al., 2013). At least three blank filters were analysed for each new batch of filters and relevant elements reference standards were checked regularly. Standard error (SE) is given for all sampling points. For calibration, detection limits, precision and accuracy see Paulino et al. (2013). The reason for using two different filter types in these analyses was to compensate for analytical interference from the elemental composition of the filters themselves. Data on C, N and P content were collected from the glass fiber filters, while data on Si, Ca, P, Mg, S, K and Fe content were collected from the polycarbonate filters. In the case of Fe, both sampling and analysis are more challenging for the soluble (nM range) than particulate fraction (μM range). Improved insight into element composition of individual bacteria was realized by application of the X-ray microanalysis (XRMA) in the electron microscope (Norland et al., 1995; Heldal et al., 1996a).

Samples for scanning electron microscopy (SEM) were made by filtering 500 mL of sea water onto 0.6 μm pore size Poretics polycarbonate filters (25 mm). The filters were air dried and stored in plastic tubes until further preparation. SEM specimens were prepared by mounting the filters on Al-stubs and coating them with Au/Pd in a

Polaron SC502 Sputter Coater for 30 s. The specimens were viewed in a Zeiss Supra 55VP or a JEOL SCM 6400 scanning electron microscope at 250–3500 × magnification or higher if necessary. Each sample was examined for composition and relative abundance of the dominating groups of microorganisms and particles. The literatures used for determination of phytoplankton were Sarno et al. (2005) and Throndsen et al. (2007).

3. Results and discussion

3.1. Hydrographical conditions, chl a and nutrients

The Raunefjord is an open fjord with close connections to the open coastal water and therefore, it is strongly influenced by the coastal circulation dynamics. Typical for western Norwegian fjords is water of Atlantic origin (salinity ≥ 35.00) being encountered below sill depth, NCCW within the intermediate layer (extending between the sill and the pycnocline; 33.00 ≤ salinity < 35.00), and above this Fjord water (FW) (salinity < 33.00) (Erga and Heimdal, 1984; Aure et al., 1996; Sætre et al., 2007). Due to the fact that water exchanges between coast and fjord is regulated by wind speed and direction, a yearly variation in both timing and species composition of phytoplankton blooms is to be expected.

3.1.1. Time series 2009–2012 Raunefjord

From Fig. 2 it can be seen that recurrent inflow/upwelling events of AW reaching depths shallower than 30 m, occurred in 2009 and 2010, with the most intense period appearing during mid-May–late July (weeks 20–30). Among these "upwelling years", 2010 emerges to be an extreme case with saline AW approaching the surface towards the end of June (Fig. 3). Even if the upper 30 m of the water column became less saline during the rest of 2010, it was less marked than for the other years (Figs. 2, 3). Typical for 2011 and 2012 were low upwelling activity and brackish water (salinity < 32) dominance over the upper 20 m of the water column, but 2011 was special in this respect, with salinities below 30 being typical for most of the year, and salinities around 28 in the upper 5–10 m over extended periods during spring, summer and autumn (Fig. 3). Another striking difference between the years was the long lasting period during winter-spring-summer 2010 with more saline water higher up in the water column (Fig. 3). This water mass was characterized by salinities > 33.00, separating it from FW with salinities ≤ 33.00 (Erga and Heimdal, 1984). Our data indicate a more or less continuous upwelling of saline deep water during the period February–June (Fig. 2). The strong upwelling of AW is also evident from the increase in nitrate and silicate concentration at 50 m in late April–early May and at 5 m in mid-June (Fig. 4a,b).

A characteristic feature of the spatial distribution of in situ chl *a*, obtained from continuous profiles of fluorescence, was, except for 2010, a deep penetrating maximum layer during late winter–early spring (mid-February–late March), in 2009 and 2011 even deeper than 50 m (Fig. 2). In the atypical year 2010, on the other hand, the spring bloom was absent and no significant algal biomass appeared before late April–early May, although we can see a decrease in nitrate and silicate concentration between week 12 and 14, probably reflecting a previous diatom bloom in this water mass before it entered the fjord. The existence of a deep maximum of 1.0–2.1 μg L^{-1} chl *a* between 47 and 51 m on 29 June 2010, is probably coupled to the ongoing inflow and upwelling of AW. Towards autumn, the chl *a* maximum layer was in general positioned closer to the surface. Yearly maximum in chl *a* ranged from 5.9 to 10.8 μg L^{-1} (values not visible from Fig. 2), which is

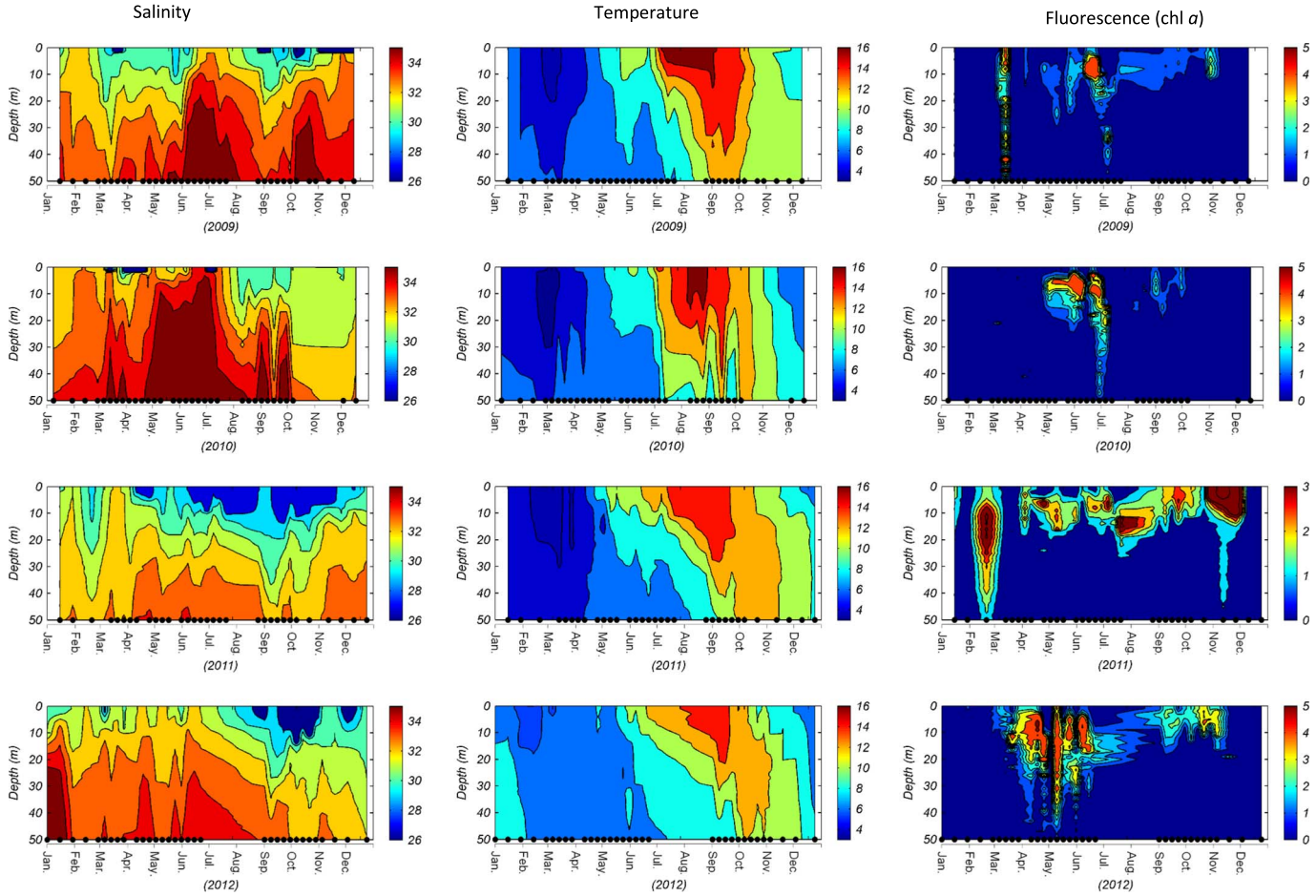

Fig. 2. Isopleth diagrams for salinity, temperature (°C), and chlorophyll *a* fluorescence (μg L^{-1}) in the Raunefjord during 2009–2012. Black dots on the x-axis indicate sampling dates.

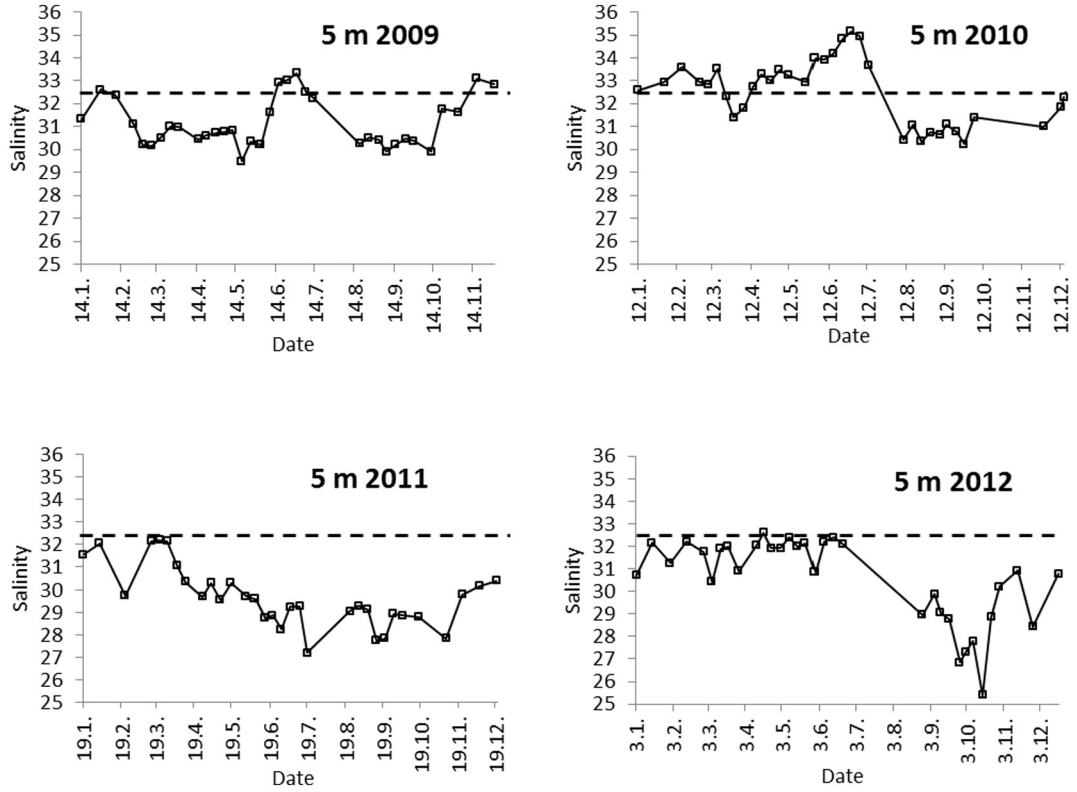

Fig. 3. Salinity at 5 m in the Raunefjord during 2009–2012. The dashed horizontal line in each graph shows the average salinity for 2010.

typical for other western Norwegian fjords as well (Erga and Heimdal, 1984; Erga, 1989; Erga et al., 2005). From our data it can also be seen that the winter - spring 2009–2010 was characterized by minimum fluorescence (chl *a*)/turbidity ratios, indicating dominance of unpigmented particles during this period, while maximum turbidity was found during phytoplankton blooms in June both in 2010 and 2011 (Fig. 5a,b), due to increasing numbers of empty diatom frustules and loose coccoliths.

3.1.2. Fedje-Shetland section February and May 2010

The inner 10 stations on the section, extending westwards from Fedje, are representative for the NCCW. They also cover the Norwegian Trench (typical depths of 300 m) (Fig. 6). The NCCW is characterized by an upper layer consisting of mixed coastal water with typical salinities below 34 overlaying the AW (Fig. 6a,b). In February a density front (i.e. a narrow zone of sharp horizontal density gradient) was situated around Stn 12, about 100 km west from the Norwegian coast (Fig. 6e), and in May it was in the upper 20 m displaced further west to Stn 13, about 110 km from the coast (Fig. 6f). The vertical extension of the brackish layer close to the coast (Fedje) decreased strongly from February to May, as demonstrated by the 34.0 isohaline ascending from 80 m to 10 m (Fig. 6a,b). This upwelling was noticeable for salinities up to 34.6, and was accompanied by a strong and persistent northerly wind field along the west coast (Fig. S1), resulting in a more westwards displacement of NCCW in May than in February. According to Sætre et al. (1988) the response time of the wind driven upwelling on the west coast of Norway is only 2–5 days after the onset of northerly wind period. It could also be seen in relation to the extremely stable high pressure systems existing during winter 2009/2010 in the adjacent North Atlantic waters, leading to a record-breaking negative NAO index (Osborn, 2011). Such a powerful combination of physical forces resulted in the strongest and most long-lasting upwelling of Atlantic deep water recorded since 1941–1942 and 1913 in the fjords around Bergen (Johannessen et al., 2010; Erga et al., 2012).

The nutrient distributions show that the highest concentrations of nitrate (Fig. S2e,f), silicate (Fig. S2i,j) and phosphate (Fig. S2g,h) were encountered at depth in the Norwegian Trench both in February and May, with a typical maximum 11, 5 and 0.7 μmol L^{-1}, respectively, giving a N:Si:P atomic ratio of 15.7:7.1:1, close to the Redfield ratio for N:P (16:1) (Redfield et al., 1963). The upper and more brackish part of the NCCW, on the other hand, was nutrient depleted in May, the outer boundary coinciding with the position of the density front (see above), where an extensive chl *a* layer had developed (Fig. S2a,b). For deep AW (300 m) silicate values around 5 μmol L^{-1} seem to be typical (Rey, 2012). It can be seen that during the period of strong offshore advection of NCCW in May, the upwelling Norwegian Trench water contained maximum nitrate, silicate and phosphate concentrations of 10, 4.5 and 0.6 μmol L^{-1}, respectively. The nitrate and silicate levels are in good accordance with those found at 50 m in the Raunefjord in May (Fig. 4a,b), revealing a continuous inflow of nutrient rich water from offshore to inshore taking place at this time.

3.2. Seasonal variations in seston elemental composition

3.2.1. Particulate C-N-P

In general, there is a good agreement between C, N and P, based on the close relation between these elements in biogenic material, with average values of 15.18 μM, 2.47 μM and 0.23 μM, respectively (Fig. 7a,b,c). Extremely low values of C; 3.6 μM, N; 0.44 μM and P; 0.051 μM were affiliated with the record-breaking negative NAO index during the winter season 2009–2010. It resulted in extremely low seston concentrations and atomic elemental ratios of C:N, C:P and N:P (Fig. 7d,e,f) mostly below the Redfield atomic ratio (C:N:P = 106:16:1). After the low biomass period there was a fast and strong increase in the elemental concentrations during the comprehensive upwelling of AW in spring – early summer, when C (57.5 μM), N (8.1 μM) and P (0.92 μM) maximum values exceeded average value with 3.8, 3.3 and 4.0 ×, respectively. It therefore seems that the AW contained seston with a higher fraction of P than N, which led to minimum C:P (39.6) and N:P (6.3) atomic ratios at this time. The C:N

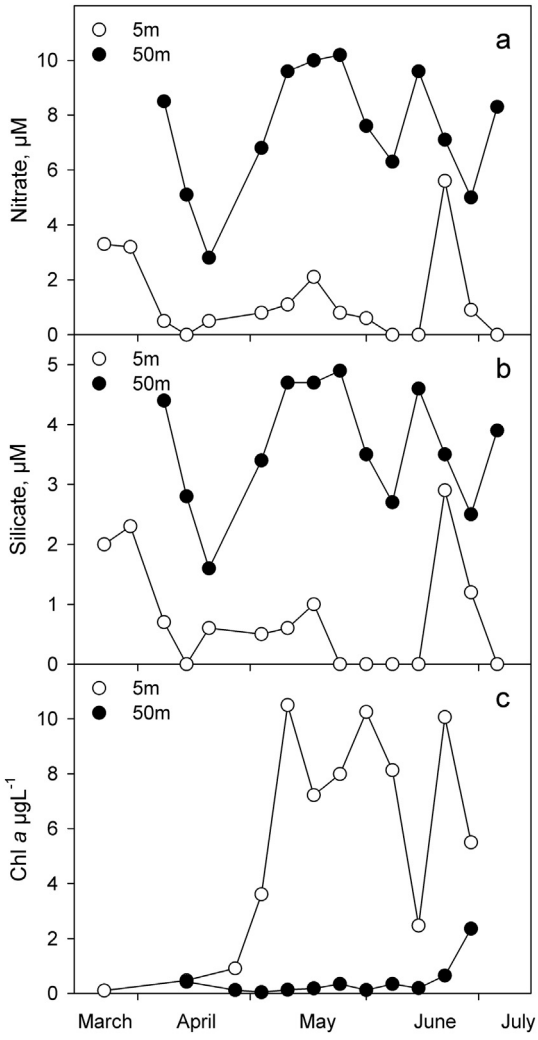

Fig. 4. Nitrate (µM) (a), silicate (µM) (b), and chlorophyll *a* (chl *a*) (µg L^{-1}) (c) at 5 and 50 m in the Raunefjord from 15 March–29 June 2010.

ratio on the other hand, was close to the Redfield ratio (6.6) during the upwelling period. Another pattern recognized was the relatively higher N values than C and P values during winter 2011, coinciding with minimum C:N (2.6) ratio and maximum N:P (33.1) ratio. Maximum C:N (12.9) and C:P (159.7) ratios were encountered in winter 2012 and early summer 2011, respectively. For the whole investigation period average values of C:N, C:P and N:P atomic ratios were 6.0, 75.2 and 13.2, respectively. According to Klausmeier et al. (2004), classical Redfield N:P ratios around 16 should be considered more as species-specific, since optimal N:P ratios for marine phytoplankton vary from 8.2 to 45.0, depending on ecological conditions.

From Figs. 2 and 7d,e it emerges that high C:N and C:P atomic ratios are associated with haline stratification and high phytoplankton biomass (chl *a*), while high N:P ratios (Fig. 7f) are more related to mixed winter conditions with low concentrations of chl *a*. In another study from coastal waters of south-eastern Norway, winter values for particulate organic C (POC), N (PON) and P (POP) were found to be below 10, 1, and 0.1 µM, respectively, which on average more than doubled during the growth season (Frigstad et al., 2011). The results are in agreement with Geider and La Roche (2002), who based on a number of published studies on elemental composition of marine phytoplankton concluded that cellular N:P atomic ratios under nutrient replete conditions ranges from 5 to 19, with most of the observations below the Redfield ratio (16). They also emphasize that the transition between N- and P- limitation for phytoplankton growth seems to be within the N:P

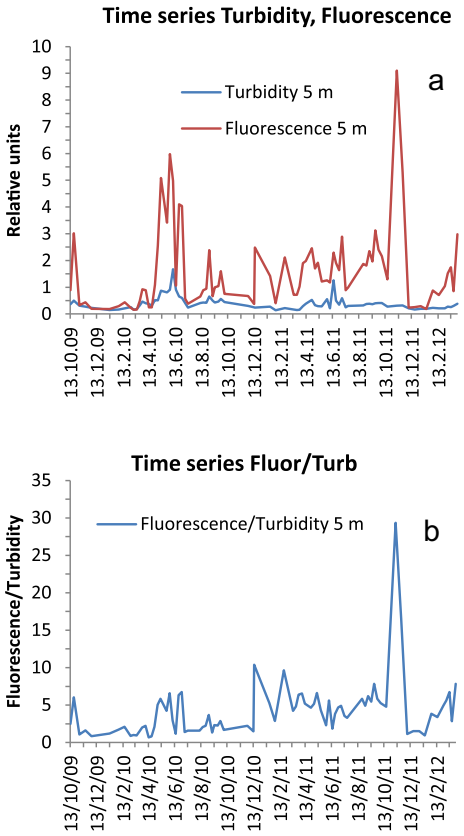

Fig. 5. Fluorescence (chl *a*) and turbidity at 5 m (a), and the fluorescence/turbidity ratio (b) at 5 m from 13 October 2009 to 19 March 2012 in the Raunefjord.

ratio range 20–50. For North Sea phytoplankton off the Norwegian west coast, Sakshaug et al. (1983) gave C:N, C:P and N:P atomic ratios in the range 6.2–19.6, 50–143, and 5.1–12, respectively, in May. Another study from the Raunefjord showed that bacteria sampled at 5 m depth in June had C:N and C:P atomic ratios of 4.5 and 45.3, respectively (Fagerbakke et al., 1996), which results in a N:P ratio of 10. According to criteria given by Paasche and Erga (1988), C:P > 200 and N:P > 20 indicates P-limitation, while C:N > 10 (Redfield = 6.6) indicates N-limitation.

Due to the fact that Scandinavian fresh water is normally characterized by a low P content, the Norwegian fjords are often found to be more P- than N-limited (Sakshaug et al., 1983; Paasche and Erga, 1988; Thingstad et al., 1993). Effluents from anthropogenic sources of N and P have been shown to have only local effects, being overridden by the large scale dilution effect caused by intensive water exchanges between coastal and fjord waters (Aure and Stigebrandt, 1990; Braaten, 1992; Ervik et al., 1997; Vogelsang et al., 2006). Altogether it seems unlikely that any severe nutrient N and/or P limitation occurred during the annual growth cycles in the Raunefjord.

3.2.2. Particulate Ca-Si

The Ca and Si elements are mostly associated with cell cover structures of coccolithophorids and diatoms, respectively, and therefore high concentrations of these elements are related to blooms of these plankton groups, but do not always follow the development pattern of elements like C, N and P, or plankton biomass in general (Paulino et al., 2013). Particulate Ca and Si varied between 0.099 and 6.28 µM, and 0.071–3.63 µM, respectively (Fig. 7g,h). For the outer Hardangerfjord average particulate Ca and Si values for the upper 50 m in April 1973 were 0.18 µM and 4.5 µM, respectively (Price and Skei, 1975).

We have no reason to believe that rivers are important sources of particulate Si in the Raunefjord, because there are no major river

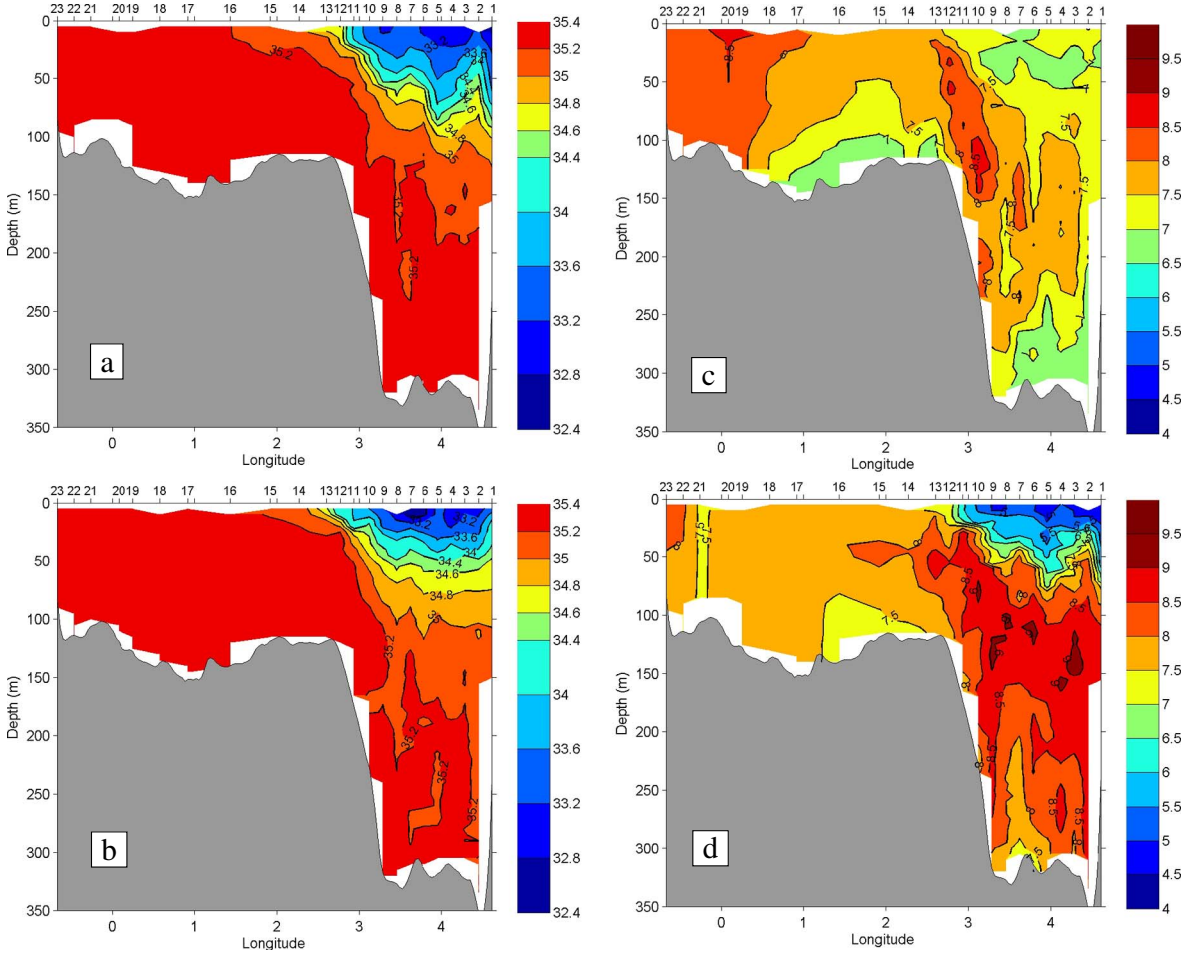

Fig. 6. Isopleth diagrams for salinity (a, b), temperature (°C) (c, d), and potential density (σ_t) (kg m^{-3}) (e, f) along the Fedje – Shetland section during 13–14 February 2010 (upper panels; a, c, e) and during 4–5 May 2010 (lower panel; b, d, f).

outlets and because the fjord is closely connected to open coastal waters. The particulate Si in the Raunefjord should hence be of biological origin, and accordingly, the maximum particulate Si concentration observed on 1 June 2010 (Fig. 7h) coincided with a bloom of the diatom *Skeletonema marinoi* (Fig. S3d, Table S1). The presence of significant amounts of diatoms at 50 m from early May to late June 2010 in the Raunefjord, beginning with *Chaetoceros* spp. (many with resting spores) and *S. marinoi* and (Fig. S3b,d), and ending with *Pseudo-nitzschia* sp. (image not shown, but see Table S1), is in compliance with the inflow and upwelling of AW at this time (see above). On the other hand, some diatom species are present in limited numbers during the whole season; one of these is the tiny *Arcocellulus cornucervis* (Fig. S3a).

Also in the case of particulate Ca, biogenic matter is probably the main source, basically in the form of coccolithophores, but also foraminifers and tintinnides (ciliate protozoans) may function as calcium carbonate accumulators by their loricae, which are often covered with coccoliths and diatom theca (Fig. S3c, Table S1) (Takahashi and Ling, 1984; Langer, 2008). Besides these, irregular inorganic calcium carbonate particles are frequently occurring (Fig. S3f). According to Heldal et al. (2012b) such particles may be quantitatively important, especially outside the coccolithophore growth season, and they represent a previously unaccounted fraction of marine calcium carbonate. They are within the size range 1–100 μm and could be formed by bacteria. In areas strongly influenced by SPM exported from glaciers, like the Kongsfjord, Svalbard, Ca values over the water column ranged between 0.04 and 2.96 μM for the period June–September 2012 (Bazzano et al., 2014).

Maximum Ca concentration (6.28 μM) was measured 8 June 2010 (Fig. 7g). An interesting pattern concerning Ca was the extended long period with impoverished values during the winter 2009–2010 and spring 2010, ahead of the *Emiliania huxleyi* bloom (Fig. S3e, Table S1), compared with all the other elements. This resulted in maximum Ca value exceeding the average by 10.8 × during the inflow of AW. For particulate Si, on the other hand, the impact of the upwelling was not that prominent, with maximum value (3.63 μM on 1 June) exceeding the average value by 4.6 ×, which is close, but somewhat higher than that found for the other macro elements P (4.0 ×), C (3.8 ×) and N (3.3 ×) (see above). In June 2010 there was an ongoing dense bloom of *E. huxleyi* also in the adjacent fjords. Based on the fact that one single coccolith contains 0.67 pg Ca ($1.67\ 10^{-8}$ μM), the Ca content of one *E. huxleyi* cell with 15 attached and 10 loosened coccoliths corresponds to $4.18\ 10^{-7}$ μM Ca (Fagerbakke et al., 1994; Paasche, 2002). In the nearby Hjeltefjord (see Fig. 1), $14.6\ 10^{6}$ cells L^{-1} of *E. huxleyi* was measured one week later (http://algeinfo.imr.no/eng/), which should add up to 6.1 μM Ca. We can therefore conclude that the peaks in particulate Ca observed in early summer is due to the coccoliths from *E. huxleyi*.

3.2.3. Particulate S-Fe-K-Mg

Particulate S and Fe varied between 0.013 and 0.46 μM, and 0.008–0.23 μM, respectively (Fig. 7i,j), with maximum value of S and Fe occurring on 8 June and 20 September 2010, respectively. Our average particulate S and Fe values compares well with earlier studies in the same area (i.e. 0.17 μM and 0.09 μM, respectively, Price and Skei, 1975), but the Fe values are 10 times lower than in the Kongsfjord (Svalbard), which is strongly influenced by terrigenous sources like glacier melting water (0.04–2.8 μM) (Bazzano et al., 2014).The

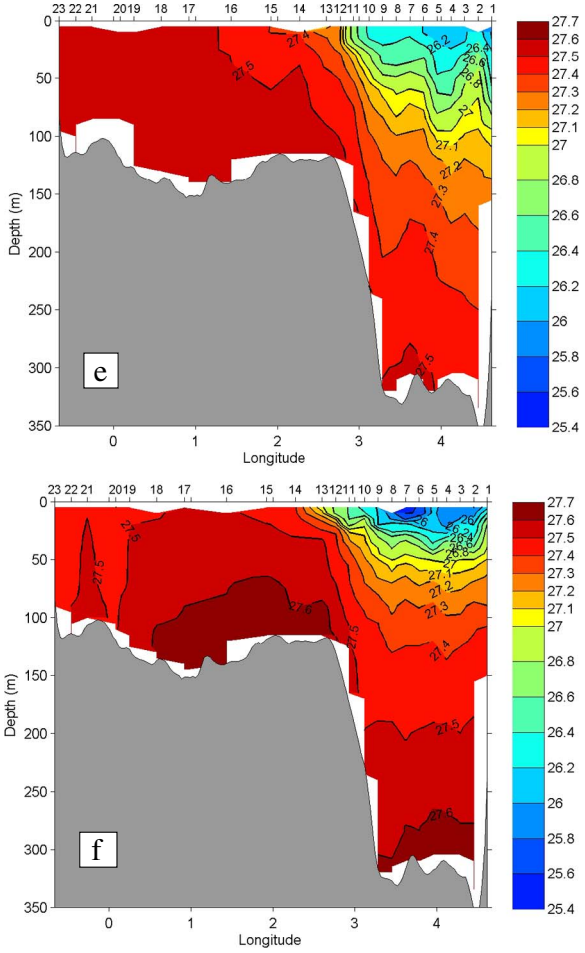

Fig. 6. (*continued*)

maximum S and Fe values in the Raunefjord exceeded the average by 5.3 and 3.3 ×, respectively. It should be noted that except for the steep increase during late spring – early summer 2010, particulate S values remained low for the whole investigation period. It therefore seems that the inflowing AW contributed strongly to the particulate S and it resulted in a C:S atomic ratio of 126:1 when both C and S reached their maximum. This is consistent with the bloom of the dimethylsulfoniopropionate (DMSP) producing *Emiliania huxleyi* (Matrai and Keller, 1994) on 8 June 2010 in the Raunefjord. According to Matrai and Keller (1994), a C:S atomic ratio of 120–130 is typical for exponentially growing *E. huxleyi* cells.

Particulate potassium and magnesium co-varied during the whole investigation period with peaks during spring and autumn, but the strongest signal was seen in connection with the Atlantic inflow during late spring – early summer 2010 (Fig. 7k,l), as found for all the other elements, except Fe. Now maximum K and Mg values reached 0.74 μM and 0.87 μM, respectively, on 1 June. According to Jaworski et al. (2003), 0.57 μM particulate K is typical for a diatom culture with cell density of 19×10^6 cells L^{-1}. Average and minimum values of K and Mg were 0.080 μM and 0.007 μM, and 0.170 μM and 0.040 μM, respectively, and compares well with earlier reports from the same area (i.e. 0.03 μM K and 0.11 μM Mg, Price and Skei, 1975). During the glacier melting season in the Kongsfjord, Svalbard, K and Mg values varied in the range 0.02–1.82 μM and 0.05–2.31 μM, respectively (Bazzano et al., 2014). Maximum values of K and Mg in the Raunefjord were 9.3 and 5.1 times the average values, respectively. It can also be seen that the value range of K and Mg are on the same level as P, and they have a similar variation pattern, except for the winter 2009–2010, when concentrations of Mg > P > K, while the main pattern was P ≥ Mg > K.

Among all the elements in our study, iron was the only one revealing no patterns in seasonal variation (Fig. 7). Particulate iron reached its maximum on 20 September 2010 when 0.22 μM was obtained (Fig. 7j), which is close to the lower value range given for coastal water of the Southern Bight in the North Sea (Schoemann et al., 1998) and the Trondheimsfjord, mid Norway (Öztürk et al., 2002), where particulate Fe values varied between 0.01 and 1 μM and 0.05–1 μM, respectively, with the highest values encountered in surface waters during spring river discharges. On the time of maximum Fe in the Raunefjord, C reached 15.1 μM, giving a C:Fe atomic ratio of 68.6 (i.e. Fe:C = 0.015:1). This is on a scale 1000 × higher than the cellular Fe:C atomic ratio of 30×10^{-6} for marine protists (based on 0.2 μm Nuclepore filters) following Fe fertilization in the Southern Ocean (Twining et al., 2008), for growth of the diatom *Thalassiosira weissflogii* under Fe-replenished and otherwise optimal conditions (Price, 2005), and for a diatom spring bloom in the Pacific Ocean, east of New Zealand (King et al., 2012). Such a big difference may be due to the presence of iron sequestering bacteria (Fig. S4a,b,c), which have been estimated to contribute with as much as 1 μg Fe L^{-1} (Heldal et al., 1996b). Average particulate Fe for our study is 0.068 μM, which is about 10 × higher than found for the North Atlantic (Barrett et al., 2012; Lam et al., 2012), but on the same level found for open waters of the Black Sea, where values around 0.03 μM (based on 1.0 μm Nuclepore filters) were found in the upper 35 m (Yiğiteran et al., 2011). For coastal waters of the southeastern US, values between 0.02 and 0.04 μM are typical (based on 0.45 μm HA filters) (Atkinson and Stefánson, 1969). The same appears to be the case for US Pacific waters (Martin and Knauer, 1973). Timmermans et al. (1998) could not find any sign of true iron deficiency for marine phytoplankton of the North Sea and northeast Atlantic Ocean.

3.2.4. Elemental correlations

Due to the complex relationships with other environmental regulation factors like light and temperature, interpretation of trace element availability/limitation and their interactions with phytoplankton growth is not straightforward (Geider and La Roche, 1994). The elemental relationships could be sorted into three groups according to decreasing order of the regression coefficient, the first group consisted of Mg-K, C-N, Mg-S, P-S, S-K, P-K, Si-K, P-Mg, N-P and C-P with r^2 decreasing from 0.94 to 0.82, the second group of C-S, Si-S, N-S, C-Si, N-Si, C-K, C-Mg, C-Ca and N-Mg with r^2 decreasing from 0.77 to 0.60, and the third group of Ca-S, N-Ca, P-Ca, Si-Fe, Ca-Mg, Ca-K, P-Fe, Si-Ca, K-Fe, Mg-Fe, N-Fe, C-Fe, S-Fe and Ca-Fe with r^2 decreasing from 0.52 to 0.17 (Table 1). The close connection between C-N, N-P and C-P is to be expected since they are related to each other by the well-known Redfield ratio. In our data set, however, the strongest correlation was found between Mg and K, which could be attributed to their common role as activators for many enzymes needed in photosynthesis and respiration (Salisbury and Ross, 1992; Taiz and Zeiger, 2006).

For Ca and Fe our data show only weak correlations with the other elements (Table 1). This could be due to the fact that the origin and biogeochemical cycles of C-N-Si-P-Mg-S-K and Ca-Fe are different, revealed by a large inorganic fraction in the pool of particulate Ca and Fe. The formation of inorganic Ca-(none-coccoliths) and Fe-particles are probably initiated by bacteria, which was often associated with these complexes. In coastal/fjord areas, strong vertical convection, characterized by interchanging upwelling and downwelling events during the season, will displace these particles upwards and downwards in the water column, respectively. Such directional changes in particle transport are essential for both the biogeochemical cycles and for the functioning of the carbon pump/ocean acidification.

3.2.5. Overall elemental ratio relationships

We have shown that the elemental concentrations of seston at 5 m depth in the Raunefjord responded strongly to inflow and upwelling of

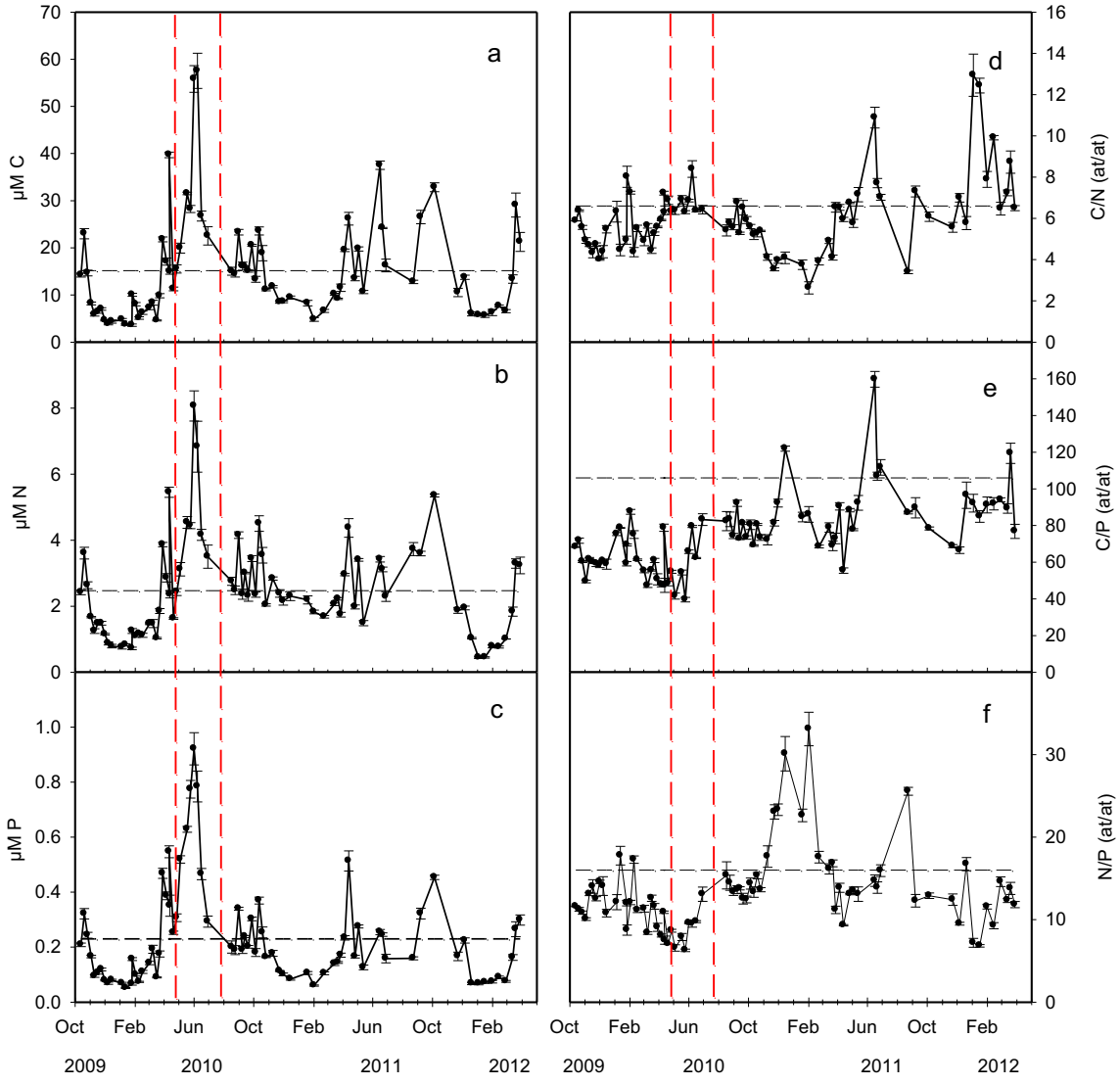

Fig. 7. Elemental composition of seston at 5 m from October 2009 to March 2012 in the Raunefjord. Carbon-C (a), nitrogen-N (b), phosphorus-P (c), C/N (d), C/P (e), N/P (f), calcium-Ca (g), silicon-Si (h), sulfur-S (i), iron-Fe (j), potassium-K (k), and magnesium-Mg (l). Average values for the time series are shown by a horizontal dashed line, in the case of the C/N, C/P and N/P ratios (at/at), the Redfield values are also shown by a horizontal dashed line. The intense upwelling period in 2010 is marked by red vertical dashed lines. (For interpretation of the references to color in this figure legend, the reader is referred to the web version of this article.)

AW in June 2010, when maximum values were obtained for all elements, except for Fe which occurred in September (Fig. 7). For our set of elements, maximum values exceeded average values with 10.8 × for Ca, 9.3 for K, 5.3 for S, 5.1 for Mg, 4.6 for Si, 4.0 for P, 3.8 for C, and 3.3 for N and Fe. This indicates that the signature of the Atlantic inflow was roughly two times stronger for Ca and K than for the others. It also points at the importance of allochthonous origin of the seston during periods of upwelling, but according to our data there are no obvious signs of crustal or geochemical origin of the inorganic fraction of the particulate metals Ca, Mg, K and Fe (see above), since most of it seems to originate from biological matter.

Based on average atomic values for each element over the whole time series and sorted according to filter type one obtain C:N:P = 66:11:1 (C:N = 6.2), and Si:Ca:P:Mg:S:K:Fe = 2.7:2:1:0.59:0.30:0.28:0.23. The C:N ratio close to Redfield and C:P and N:P below Redfield is consistent with sufficient dissolved inorganic N-nutrients and surplus P-nutrients in the Raunefjord. According to Martiny et al. (2013) there is a clear latitudinal trend in the C:N:P (at/at) ratio, decreasing from lower to higher latitudes, and they give 78:13:1 as typical for high-latitude nutrient rich waters. Combining the two sets one gets the following formula: $C_{66}N_{11}Si_{3.4}Ca_{2.3}P_1Mg_{0.73}S_{0.37}K_{0.35}Fe_{0.30}$. Among the few published works including elements beyond the classical C:N:P elemental composition is the one of Ho et al. (2003), who studied the elemental composition for a number of culture species representing the most common classes of marine phytoplankton. For whole cells they give an average of: $C_{147}N_{16}$ Ca_{23} P_1 $Mg_{0.56}$ $S_{1.3}K_{1.7}Fe_{0.0075}$, for all the species. The high Ca was explained to be due to the influence of the coccoliths. In total, the difference between our data and Ho et al. (2003) could be explained by contribution from heterotrophic microorganisms in the Raunefjord, causing the C:N:P ratio to be reduced. In accordance with this view Vrede et al. (2002) obtained an average C:N:P atomic ratio of 45:7.4:1 for bacteria isolated from the Raunefjord. In the study of Bates et al. (1994), the content of C and N in particulate matter from northeast Pacific surface waters was compared with S. They found a C:N:S atomic ratio of 182:27:1, which reveals a significant footprint from phytoplankton, and is very close to 177:29:1 calculated for the Raunefjord (based on average values).

Our data show that levels of the dissolved inorganic nutrients N (mostly nitrate), Si (silicate) and P (phosphate) around 10–12 μM, 4–5 μM and 0.7–1 μM, respectively, are typical for both deeper fjord water and NCCW (Fig. 4a,b, Fig. S1S1e–j). They are also similar to the levels encountered in deeper AW (Rey, 2012; Erga et al., 2014). It

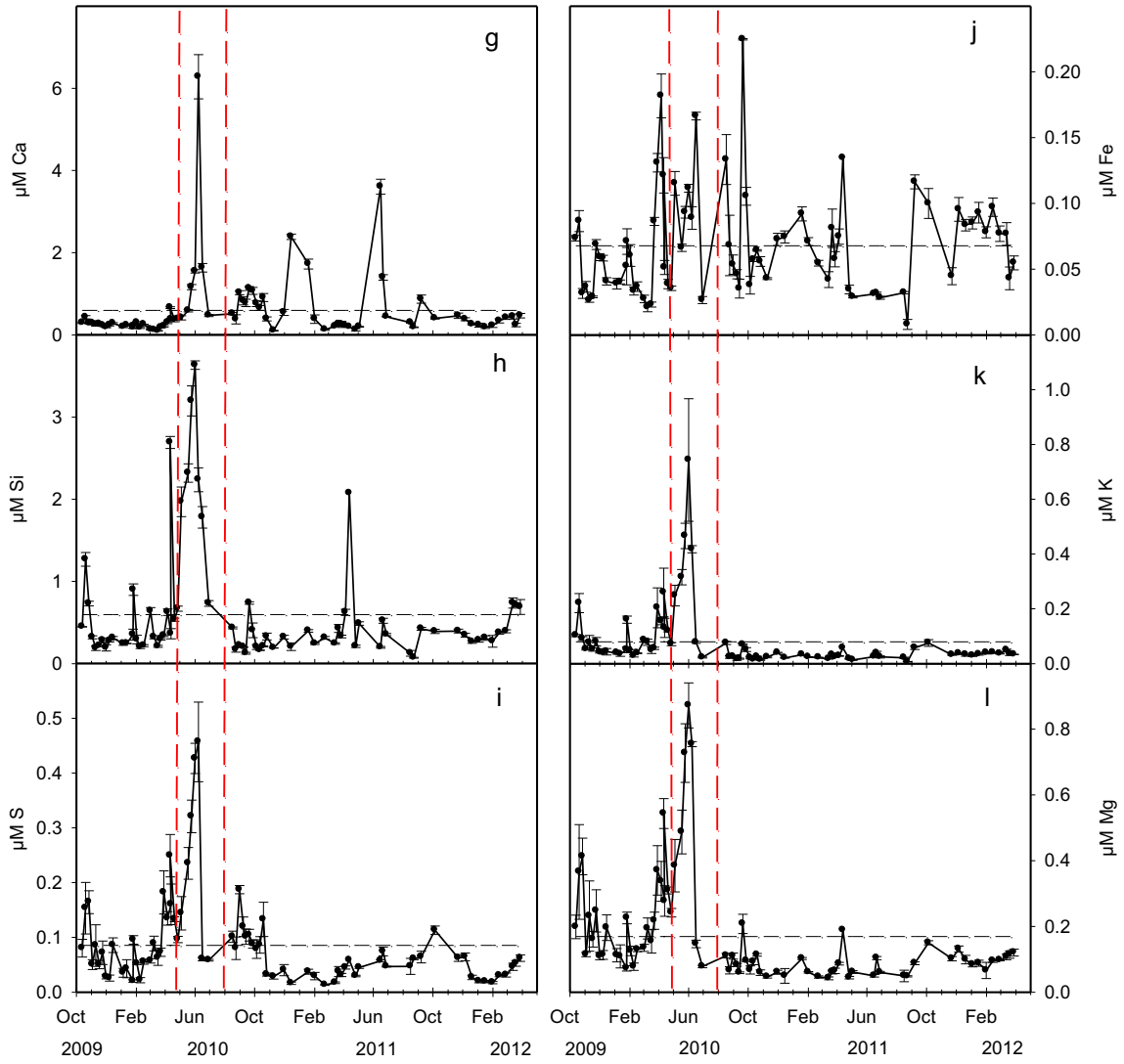

Fig. 7. (*continued*)

Table 1
Correlation matrix of different elements (at/at) in seston from 5 m depth in the Raunefjord, 2009–2012. Regressions (r^2) between C, N and P are based on material collected on GFF filters (n = 77), and between Si, Ca, P, Mg, S, K, and Fe are based on 0.6 µm PC filters (n = 75) (value range of correlations; $p < 0.01$).

	C	N	Si	Ca	P	Mg	S	K	Fe
C	1	0.94	0.71	0.63	0.82	0.64	0.77	0.66	0.30
N	0.94	1	0.68	0.51	0.82	0.60	0.75	0.63	0.31
Si	0.71	0.68	1	0.33	0.88	0.84	0.76	0.87	0.40
Ca	0.63	0.51	0.33	1	0.42	0.37	0.53	0.36	0.17
P	0.82	0.82	0.88	0.42	1	0.85	0.91	0.88	0.36
Mg	0.64	0.60	0.84	0.37	0.85	1	0.92	0.94	0.32
S	0.77	0.75	0.76	0.53	0.91	0.92	1	0.89	0.26
K	0.66	0.63	0.87	0.36	0.88	0.94	0.89	1	0.32
Fe	0.30	0.31	0.40	0.17	0.36	0.32	0.26	0.32	1

therefore seems that there is a fairly good stoichiometric match between the dissolved and particulate fraction of these elements in waters of Atlantic origin, indicating a strong influence of AW at our study site. Averaged over time there is a 1.5 × higher molar fraction of Si than Ca contained in seston from the Raunefjord, which emphasizes the predominance of diatoms over coccolithophorids and confirm their environmental fitness. With respect to climate change/ocean acidification this bias will probably be worsened, since enhanced carbon dioxide levels are supposed to impede calcification and therefore reduce growth of coccolithophorids. On the other hand, decreasing Si levels in North Atlantic water (Rey, 2012) also makes the future success of diatoms more uncertain. We believe, however, that the effect of climate change in Norwegian coastal waters, in the sense of ocean acidification and access to nutrients, will be strongly dependent on how the high pressure and low pressure systems develops (i.e. NAO index), since they play a pivotal role for the direction of the wind driven convection (i.e. upwelling or downwelling).

4. Conclusion

Extremely low seston concentrations in the Raunefjord coincided with the record-breaking negative NAO index during the winter season 2009–2010 and no phytoplankton spring bloom appeared in 2010. Later, during spring-early summer 2010, high saline water ascended closer to the surface than normal. During this period a comprehensive upwelling took place in the fjord coinciding with maximum value of the seston elements C, N, Si, Ca, P, Mg, S, K, but not for Fe. The peaks typically exceeded average values by 3.3–10.8 times, but the strongest response was seen for K and Ca. The seston at this time also contained a relatively higher fraction of P than N, resulting in minimum C:P (39.6) and N:P (6.3) atomic ratios, which are far below the Redfield ratio of 106 and 16, respectively. The C:N ratio on the other hand, was close to the Redfield ratio (6.6) during the upwelling period. Among the

elements, the strongest correlation (r^2 in decreasing order from 0.94 to 0.82) was found between Mg-K, C-N, Mg-S, P-S, S-K, P-K, Si-K, P-Mg, N-P and C-P for the whole period of investigation. Based on average values of the elements, the following overall stoichiometric relationship was obtained: $C_{66}N_{11}Si_{3.4}Ca_{2.3}P_1Mg_{0.73}S_{0.37}K_{0.35}Fe_{0.30}$. The reduced C:N:P ratio could be explained by a higher contribution of heterotrophic microorganisms. Altogether it seems unlikely that any severe nutrient N and/or P limitation occurred during the annual growth cycles in the Raunefjord. Contrary to what has been shown for some other oceanic sites, our data do not show that Fe is limiting primary production in western Norwegian coastal waters. However, a large part of the Fe-pool is probably bound up in Fe-sequestering bacteria, which could at times influence the availability of the dissolved component of the element. The impact of terrigenous sources in this context is probably low. Despite its quantitative role, Ca is together with Fe only weakly correlated with the other elements, indicating a difference in biogeochemical cycling of these two elements compared with the others. We have shown that some fraction of the inorganic particles containing Fe or Ca occurs in a variety of different forms and that they are often associated with bacteria. Due to wind driven directional changes in vertical convection during the seasons, the impact of climate change on seston composition in surface coastal waters will depend on whether the physical forcing generates upwards or downwards transport. This will also be decisive for the effect of the carbon pump/ocean acidification and biogeochemical cycling.

Supplementary data to this article can be found online at http://dx.doi.org/10.1016/j.marchem.2017.07.001.

Acknowledgements

This work was supported by the Research Council of Norway projects MERCLIM (No. 184860) and MicroPolar (No. 225956/E10), the ERC project MINOS (No. 250254) and the EU project OCEAN-CERTAIN (FP7-ENV-2013-6.1-1; No. 603773). Thanks are due to Tomas Sørlie for help with sampling CTD data, Egil Severin Erichsen for his assistance during the electron microscopy work, and Karen Gjertsen at the Institute of Marine Research for drawing the map of the investigation area.

References

Arrigo, K.R., 2005. Marine microorganisms and global nutrient cycles. Nature 437, 349–355.
Atkinson, L.P., Stefánson, U., 1969. Particulate Al and Fe in sea water off the southeastern coast of the United States. Geochim. Cosmochim. Acta 33, 1449–1453.
Aure, J., Stigebrandt, A., 1990. Quantitative estimates of eutrophication effects on fjords of fish farming. Aquaculture 90, 135–156.
Aure, J., Molvær, J., Stigebrandt, A., 1996. Observations of inshore water exchange forced by a fluctuating offshore density field. Mar. Pollut. Bull. 33, 112–119.
Barrett, P.M., Resing, J.A., Buck, N.J., Buck, C.S., Landing, W.M., Measures, C.I., 2012. The trace element composition of suspended particulate matter in the upper 1000 m of the eastern North Atlantic Ocean: A16N. Mar. Chem. 142–144, 41–53.
Bates, T.S., Kiene, R.P., Wolfe, G.V., Matrai, P.A., Chavez, F.P., Buck, K.R., Blomquist, B.W., Cuhel, R.L., 1994. The cycling of sulfur in surface seawater of the northeast Pacific. J. Geophys. Res. 99, 7835–7843.
Bazzano, A., Rivaro, P., Soggia, F., Ardini, F., Grotti, M., 2014. Anthropogenic and natural sources of particulate trace elements in the coastal marine environment of Kongsfjorden, Svalbard. Mar. Chem. 163, 28–35.
von Bodungen, B., Antia, A., Bauerfeind, E., Haupt, O., Koeve, W., Peeken, I., Peinert, R., Reitmeier, S., Thomsen, C., Voss, M., Wunsch, M., Zeller, U., Zeitschel, B., 1995. Pelagic processes and vertical flux of particles: an overview over a long term comparative study in the Norwegian Sea and Greenland Sea. Geogr. Rundsch. 84 (1), 1–27.
Braaten, B., 1992. Impact of pollution from aquaculture in six Nordic countries: release of nutrients, effects and waste water treatment. In: Aquaculture and the Environment, European Aquaculture Society Special Publication No 16, pp. 79–102.
Bratbak, G., Heldal, M., Thingstad, T.F., Riemann, B., Haslund, O.H., 1992. Incorporation of viruses into the budget of microbial C-transfer. A first approach. Mar. Ecol. Prog. Ser. 83, 273–280.
Buchan, A., LeCleir, G.R., Gulvik, C.A., González, J.M., 2014. Master recyclers: features and functions of bacteria associated with phytoplankton blooms. Nat. Rev. Microbiol. 12, 686–698.
Cranford, P.J., Hargrave, B.T., 1994. In situ time-series measurements of ingestion and absorption rates of suspension-feeding bivalves: *Placopecten magellanicus*. Limnol. Oceanogr. 39, 730–738.
Erga, S.R., 1989. Ecological studies on the phytoplankton of Boknafjorden, western Norway. I. The effect of water exchange processes and environmental factors on temporal and vertical variability of biomass. Sarsia 74, 161–176.
Erga, S.R., Heimdal, B.R., 1984. Ecological studies on the phytoplankton of Korsfjorden, western Norway. The dynamics of a spring bloom seen in relation to hydrographical conditions and light regime. J. Plankton Res. 6, 67–90.
Erga, S.R., Aursland, K., Frette, Ø., Hamre, B., Lotsberg, J.K., Stamnes, J.J., Aure, J., Rey, F., Stamnes, K., 2005. UV transmission in Norwegian marine waters: controlling factors and possible effects on primary production and vertical distribution of phytoplankton. Mar. Ecol. Prog. Ser. 305, 79–100.
Erga, S.R., Ssebiyonga, N., Frette, Ø., Hamre, B., Aure, J., Strand, Ø., Strohmeier, T., 2012. Dynamics of phytoplankton distribution and photosynthetic capacity in a western Norwegian fjord during coastal upwelling: effects on optical properties. Estuar. Coast. Shelf Sci. 97, 91–103.
Erga, S.R., Ssebiyonga, N., Hamre, B., Frette, Ø., Hovland, E., Hancke, K., Drinkwater, K., Rey, F., 2014. Environmental control of phytoplankton distribution and photosynthetic performance at the Jan Mayen Front in the Norwegian Sea. J. Mar. Syst. 130, 193–205.
Ervik, A., Hansen, P.A., Aure, J., Stigebrandt, A., Johannessen, P., Jahnsen, T., 1997. Regulating the local environmental impact of intensive marine fish farming I. The concept of the MOM system (Modelling–Ongrowing fish farms –Monitoring). Aquaculture 158, 85–94.
Fagerbakke, K.M., Heldal, M., Norland, S., Heimdal, B.R., Båtvik, H., 1994. *Emiliania huxleyi*. Chemical composition and size of coccoliths from enclosure experiments and a Norwegian fjord. Sarsia. 79, 349–355.
Fagerbakke, K.M., Heldal, M., Norland, S., 1996. Content of carbon, nitrogen, oxygen, sulfur and phosphorus in native aquatic and cultured bacteria. Aquat. Microb. Ecol. 10, 15–27.
Fomba, K., Müller, K., van Pinxteren, D., Poulain, L., van Pinxteren, M., Herrmann, H., 2014. Long-term chemical characterization of tropical and marine aerosols at the Cape Verde Atmospheric Observatory (CVAO) from 2007 to 2011. Atmos. Chem. Phys. 14, 8883–8904.
Frigstad, H., Andersen, T., Hessen, D.O., Naustvoll, L.J., Johnsen, T.M., Bellerby, R.G.J., 2011. Seasonal variation in marine C:N:P stoichiometry: can the composition of seston explain stable Redfield ratios? Biogeosciences 8, 2917–2933.
Geider, R.J., La Roche, J., 1994. The role of iron in phytoplankton photosynthesis, and the potential for iron-limitation of primary productivity in the sea. Photosynth. Res. 39, 275–301.
Geider, R.J., La Roche, J., 2002. Redfield revisited: variability of C:N:P in marine microalgae and its biochemical basis. Eur. J. Phycol. 37, 1–17.
Giordano, M., Norici, A., Hell, R., 2005. Sulfur and phytoplankton: acquisition, metabolism and impact on the environment. New Phytol. 166, 371–382.
Haines, T.H., 1973. Halogen- and sulfur-containing lipids of *Ochromonas*. Annu. Rev. Microbiol. 27, 403–412.
Heldal, M., Norland, S., Fagerbakke, K.M., Thingstad, F., Bratbak, G., 1996a. The elemental composition of bacteria: a signature of growth conditions? Mar. Pollut. Bull. 33, 3–9.
Heldal, M., Fagerbakke, K.M., Tuomi, P., Bratbak, G., 1996b. Abundant populations of iron and manganese sequestering bacteria in coastal water. Aquat. Microb. Ecol. 11, 127–133.
Heldal, M., Norland, S., Erichsen, E.S., Sandaa, R.-A., Larsen, A., Thingstad, F., Bratbak, G., 2012a. Mg^{2+} as an indicator of nutritional status in marine bacteria. ISME J. 6, 524–530.
Heldal, M., Norland, S., Erichsen, E.S., Thingstad, F., Bratbak, G., 2012b. An unaccounted fraction of marine biogenic $CaCO_3$ particles. PLoS One 7, 1–6.
Ho, T.-Y., Quigg, A., Finkel, Z.V., Milligan, A.J., Wyman, K., Falkowski, P.G., Morel, F.M.M., 2003. The elemental composition of some marine phytoplankton. J. Phycol. 39, 1145–1159.
Jaworski, G.H.M., Talling, J.F., Heaney, S.J., 2003. Potassium dependence and phytoplankton ecology: an experimental study. Freshw. Biol. 48, 833–840.
Johannessen, P., Sætre, R., Kryvi, H., Hjelle, H. (Eds.), 2010. Bergensfjordene - natur og bruk. J. Grieg forlag, Bergen, Norway.
King, A.L., Sañudo-Wilhelmy, S.A., Boyd, P.W., Twining, B.S., Wilhelm, S.W., Breene, C., Ellwood, M.J., Hutchins, D.A., 2012. A comparison of biogenic iron quotas during a diatom spring bloom using multiple approaches. Biogeosciences 9, 667–687.
Klausmeier, C.A., Litchman, E., Daufresne, T., Levin, S.A., 2004. Optimal nitrogen-to-phosphorus stoichiometry of phytoplankton. Nature 429, 171–174.
Kolber, Z., Barber, R.T., Coale, K.H., Fitzwater, S.E., Greene, R.M., Johnson, K.S., Lindley, S., Falkowski, P.G., 1994. Iron limitation of phytoplankton photosynthesis in the equatorial Pacific Ocean. Nature 371, 145–149.
Lam, P.J., Ohnemus, D.C., Marcus, M.A., 2012. The speciation of marine particulate iron adjacent to active and passive continental margins. Geochim. Cosmochim. Acta 80, 108–124.
Lange, C.B., Weinheimer, A.L., Reid, F.M.H., Thunell, R.C., 1997. Sedimentation patterns of diatoms, radiolarians, and silicoflagellates in Santa Barbara Basin, California. CalCOFI Rep. 38, 161–170.
Langer, M.R., 2008. Assessing the contribution of foraminiferan protists to global ocean carbonate production. J. Eukaryot. Microbiol. 55, 163–169.
Larsen, A., Flaten, G.A.F., Sandaa, R.A., Castberg, T., Thyrhaug, R., Erga, S.R., Jaquet, S., Bratbak, G., 2004. Spring phytoplankton bloom in Norwegian coastal waters: microbial community dynamics, succession and diversity. Limnol. Oceanogr. 49, 180–190.
Martin, J.H., Knauer, G.A., 1973. The elemental composition of plankton. Geochim. Cosmochim. Acta 37, 1639–1653.

Martin, D.D., Ciulla, R.A., Roberts, M.F., 1999. Osmoadaptation in archaea. Appl. Environ. Microbiol. 65, 1815–1825.
Martiny, A.C., Pham, C.T.A., Primeau, F.W., Vrugt, J.A., Moore, J.K., Levin, S.A., Lomas, M.W., 2013. Strong latitudinal patterns in the elemental ratios of marine plankton and organic matter. Nat. Geosci. 6, 279–283.
Matrai, P.A., Keller, M.D., 1994. Total organic sulfur and dimethylsulfoniopropionate in marine phytoplankton: intracellular variations. Mar. Biol. 119, 61–68.
Navaro, J.M., Thompson, R.J., 1995. Seasonal fluctuations in the size spectra, biochemical composition and nutritive value of the seston available to a suspension-feeding bivalve in a subarctic environment. Mar. Ecol. Prog. Ser. 125, 95–106.
Norland, S., Fagerbakke, K.M., Heldal, M., 1995. Light element analysis of individual bacteria by X-ray microanalysis. Appl. Environ. Microbiol. 61, 1357–1362.
Osborn, T.J., 2011. Winter 2009/2010 temperatures and a record-breaking North Atlantic Oscillation index. Weather 66, 19–21.
Öztürk, M., Steinnes, E., Sakshaug, E., 2002. Iron speciation in the Trondheim Fjord from the perspective of iron limitation for phytoplankton. Estuar. Coast. Shelf Sci. 55, 197–212.
Paasche, E., 2002. A review of the coccolithophorid *Emiliania huxleyi* (Prymnesiophyceae), with particular reference to growth, coccolith formation, and calcification-photosynthesis interactions. Phycologia 40, 503–529.
Paasche, E., Erga, S.R., 1988. Phosphorus and nitrogen limitation of phytoplankton in the inner Oslofjord (Norway). Sarsia 73, 229–243.
Parsons, T.R., Maita, Y., Lalli, C.M. (Eds.), 1992. A Manual of Chemical and Biological Methods for sea Water Analysis. Pergamon Press, New York.
Paulino, A.I., Heldal, M., Norland, S., Egge, J.K., 2013. Elemental stoichiometry of marine particulate matter measured by wavelength dispersive X-ray fluorescence (WDXRF). J. Mar. Biol. Assoc. U. K. 93, 1–12.
Price, N.M., 2005. The elemental stoichiometry and composition of an iron-limited diatom. Limnol. Oceanogr. 50, 1159–1171.
Price, N.B., Skei, J.M., 1975. Areal and seasonal variations in the chemistry of suspended particulate matter in a deep water fjord. Estuar. Coast. Mar. Sci. 3, 349–369.
Redfield, A.C., Ketchum, B.H., Richards, F.A., 1963. The influence of organisms on the composition of seawater. In: Hill, M.N. (Ed.), The Sea. Vol. 2. Interscience, New York, USA, pp. 26–77.
Rey, F., 2012. Declining silicate concentrations in the Norwegian and Barents Seas. ICES J. Mar. Sci. 69, 208–212.
Rey, F., Noji, T.T., Miller, L.A., 2000. Seasonal phytoplankton development and new production in the central Greenland Sea. Sarsia 85, 329–344.
Sætre, R., Aure, J., Ljøen, R., 1988. Wind effects on the lateral extension of the Norwegian Coastal Water. Cont. Shelf Res. 8, 239–253.
Sætre, R., Gjertsen, K., Bröker, K. (Eds.), 2007. The Norwegian Coastal Current: Oceanography and Climate. Tapir Academic Press, Trondheim, Norway.
Sakshaug, E., Andresen, K., Myklestad, S., Olsen, Y., 1983. Nutrient status of phytoplankton communities in Norwegian waters (marine, brackish, and fresh). J. Plankton Res. 5, 175–196.
Salisbury, F.B., Ross, C.W. (Eds.), 1992. Plant Physiology, 4th edition. Wadsworth, Inc., Belmont, California, USA.
Sarno, D., Kooistra, W.H.C.F., Medlin, L.K., Percopo, I., Zingone, A., 2005. Diversity in the genus *Skeletonema* (Bacillariophyceae). II. An assessment of the taxonomy of *S. costatum*-like species with the description of four new species. J. Phycol. 41, 151–176.
Schoemann, V., de Baar, H.J.W., de Jong, J.T.M., Lancelot, C., 1998. Effects of phytoplankton blooms on the cycling of manganese and iron in coastal waters. Limnol. Oceanogr. 43, 1427–1441.
Seeber, F., 2002. Biogenesis of iron-sulphur clusters in amitochondriate and apicomplexan protists. Int. J. Parasitol. 32, 1207–1217.
Sicko-Goad, L., Stoermer, E.F., Ladewski, B.G., 1977. A morphometric method for correcting phytoplankton cell volume estimates. Protoplasma 93, 147–163.
Stabholz, M., Durrieu de Madron, X., Canals, M., Khripounoff, A., Taupier-Letage, I., Testor, P., Heussner, S., Kerhervé, P., Delsaut, N., Houpert, L., Lastras, G., Dennielou, B., 2013. Impact of open-ocean convection on particle fluxes and sediment dynamics in the deep margin of Gulf of Lions. Biogeosciences 10, 1097–1116.
Sterner, R.W., Hessen, D.O., 1994. Algal nutrient limitation and the nutrition of aquatic herbivores. Annu. Rev. Ecol. Syst. 25, 1–29.
Taiz, L., Zeiger, E. (Eds.), 2006. Plant Physiology, 4th edition. Sinauer Associates, Inc., Publishers, Sunderland, Massachusetts, USA.
Takahashi, K., Ling, H.Y., 1984. Particle selectivity of pelagic tintinnid agglutination. Mar. Micropaleontol. 9, 87–92.
Thingstad, T.F., Skjoldal, E.F., Bohne, R.A., 1993. Phosphorus cycling and algal-bacterial competition in Sandsfjord, western Norway. Mar. Ecol. Prog. Ser. 99, 239–259.
Throndsen, J., Hasle, G.R., Tangen, K. (Eds.), 2007. Phytoplankton of Norwegian Coastal Waters. Almater forlag AS, Oslo, Norway.
Timmermans, K.R., Gledhill, M., Nolting, R.F., Veldhuis, M.J.W., de Baar, H.J.W., van den Berg, C.M.G., 1998. Responses of marine phytoplankton in iron enrichment experiments in the northern North Sea and northeast Atlantic Ocean. Mar. Chem. 61, 229–242.
Tůma, J., Skalický, M., Bláhová, P., Rosůlková, M., 2004. Potassium, magnesium and calcium content in individual parts of *Phaseolus vulgaris* L. plant as related to potassium and magnesium nutrition. Plant Soil Environ. 50, 18–26.
Twining, B.S., Baines, S.B., Vogt, S., de Jonge, M.D., 2008. Exploring ocean biogeochemistry by single-cell microprobe analysis of protist elemental composition. J. Eukaryot. Microbiol. 55, 151–162.
Vogelsang, C., Grung, M., Jantsch, T.G., Tollefsen, K.E., Liltved, H., 2006. Occurrence and removal of selected organic micropollutants at mechanical, chemical and advanced wastewater treatment plants in Norway. Water Res. 40, 3559–3570.
Vrede, K., Heldal, M., Norland, S., Bratbak, G., 2002. Elemental composition (C:N:P) and cell volume of exponentially growing and nutrient-limited bacterioplankton. Appl. Environ. Microbiol. 68, 2965–2971.
Wells, M.L., Price, N.M., Bruland, K.W., 1995. Iron chemistry in seawater and its relationship to phytoplankton: a workshop report. Mar. Chem. 48, 157–182.
Westbroek, P., Brown, C.W., Bleijswijk, J.D.L., van Brownlee, C., Brummer, G.J., Conte, M., Egge, J., Fernandez, E., Jordan, R., Knappertsbusch, M., Stefels, J., Veldhuis, M.J.W., Wal, P., van der Young, J., 1993. A model system approach to biological climate forcing: the example of *Emiliania huxleyi*. Glob. Planet. Chang. 8, 27–46.
Yiğiteran, O., Murray, J.W., Tuğrul, S., 2011. Trace metal composition of suspended particulate matter in the water column of the Black Sea. Mar. Chem. 126, 2017–2228.
Zwolsman, J.J.G., van Eck, G.T.M., 1999. Geochemistry of major elements and trace metals in suspended matter of the Scheldt estuary, southwest Netherlands. Mar. Chem. 66, 91–111.